Compensation of Current Measurement Error for Current-Controlled PMSM Drives

Myoungho Kim, *Member, IEEE*, Seung-Ki Sul, *Fellow, IEEE*, and Junggi Lee, *Member, IEEE*

***Abstract*—Accurate measurement of phase current is crucial in a current-controlled permanent-magnet synchronous machine (PMSM) drive system. Current measurement error directly deteriorates torque control performance. This paper analyzes effects of the current measurement error on the phase current and the output voltage of the current controller. Based on the analysis, a compensation method is proposed. The proposed method compensates the offset and scaling errors separately without any additional hardware but using the commanded voltage reference of the current controller. The proposed method can be applied to general current-controlled PMSM drives in the whole operation range. Experimental results verify the effectiveness of the proposed compensation method.**

***Index Terms*—Current measurement, electric current control, machine vector control, motor drives, permanent-magnet motors.**

NOMENCLATURE

i_{xs_mea}	$x(a, b,$ or $c)$-phase measured current.
i_{xs}	$x(a, b,$ or $c)$-phase real current.
I_{xs_off}	$x(a, b,$ or $c)$-phase current offset error.
K_x	$x(a, b,$ or $c)$-phase current measurement scaling gain.
Δi_{xs}	$x(a, b,$ or $c)$-phase current measurement error.
$i^e_{xs\_\mathrm{mea}}$	Synchronous $x(d$ or $q)$-axis measured current.
i^e_{xs}	Synchronous $x(d$ or $q)$-axis real current.
Δi^e_{xs}	Synchronous $x(d$ or $q)$-axis current measurement error.
v^e_{xs}	Synchronous $x(d$ or $q)$-axis motor terminal voltage.
Δv^e_{xs}	Synchronous $x(d$ or $q)$-axis voltage error.
θ_e	Electrical angle.

I. INTRODUCTION

PRECISE measurement of stator currents is crucial in the vector control of ac machine drives [1]. The current measurement error causes not only transient but also steady-state error on the stator currents. Both could directly deteriorate torque control performance and result in torque nonlinearity, ripple torque, and additional losses due to the ripple current and torque [2].

The current measurement path consists of several components, such as Hall sensors, matching circuits, noise filter circuits, and analog–digital (A/D) converters [1]. One or more of the components may affect the measurement error by various factors such as device tolerance, temperature drift, aging, and noise. Even in a well-tuned measurement system, small amount of error is inevitable. In addition, the aspect of the measurement error could vary with time. Therefore, the measurement error should be compensated periodically or consistently.

Many researches have been conducted for the current measurement error compensation [3]–[8]. The offset of the measurement can be simply cancelled by compensating the stored offset value, which is measured when the inverter is stopped [3]. This method has been adopted widely for the general inverter system. However, it did not compensate the scaling error and the variation of the offset during the operation. In [4], offset of the phase current is detected by monitoring the ac component at the dc-link current. However, it requires additional current sensor at the dc link and cannot detect the scaling error. A compensation method based on the speed ripple detects the speed ripple caused by the current measurement error and suppresses it by modifying the torque command of the speed controller [5]. This method requires mechanical parameters and is only able to be adopted to the drive system where the speed is regulated. Since the torque ripple caused by the current measurement error is periodic, an iterative learning method can be used to suppress it [6]. However, in [5] and [6], the speed or torque was compensated by modifying the commands of the controller. They do not compensate the current measurement error itself. A high-frequency voltage injection method can be used regardless of a speed control structure [7]. However, the high-frequency signal injection is not permitted in some applications because of additional losses and acoustic noises. Reference [8] showed the effect of the current measurement scaling error and presented a compensation strategy. However, this method considered a system that employs three phase current sensors and cannot be used for a system with two current sensors. Studies in [9]–[11] used the commanded voltage reference of the current controller to compensate the current measurement error. However, their compensation methods were limited in terms of operating speed or load condition. In [12], it had been reported how the ac machine drive system could be operated under failure of one of the current sensors. The faulted sensor is detected by applying test voltage signals, and an observer starts estimating the currents.

Manuscript received April 11, 2013; revised September 4, 2013 and December 2, 2013; accepted December 28, 2013. Date of publication January 21, 2014; date of current version September 16, 2014. Paper 2013-IDC-182.R2, presented at the 2012 IEEE Energy Conversion Congress and Exposition, Raleigh, NC, USA, September 15–20, and approved for publication in the IEEE TRANSACTIONS ON INDUSTRY APPLICATIONS by the Industrial Drives Committee of the IEEE Industry Applications Society.

M. Kim is with the Power and Control Division, Samsung Heavy Industries, Hwasung 445-330, Korea (e-mail: myungho1.kim@samsung.com).

S.-K. Sul is with the Department of Electrical Engineering and Computer Science, Seoul National University, Seoul 151-742, Korea (e-mail: sulsk@plaza.snu.ac.kr).

J. Lee is with the Power Electronics Team, LG Electronics, Incheon 405-852, Korea (e-mail: Jungi.lee@lge.com).

Color versions of one or more of the figures in this paper are available online at http://ieeexplore.ieee.org.

Digital Object Identifier 10.1109/TIA.2014.2301873

However, this is a strategy for the case when the current sensor is completely broken and does not provide a compensation strategy for minor faults such as scaling or offset error.

This paper analyzes effects of the current measurement error for a general current-controlled permanent-magnet synchronous machine (PMSM) drive system, which uses two current sensors. Effects of the current measurement error on the current and commanded voltage reference of the current controller are presented. Based on the analysis, a compensation strategy is proposed. The proposed method is implemented in software and does not require any additional hardware. In addition, it is applicable to general PMSM drive systems without limitation of operation range. Experimental results are presented to verify the proposed algorithm.

II. Effects of Current Measurement Error

Current measurement error can be generally classified into two categories, i.e., offset and scaling errors. The offset of the measurement is a superimposed value on the actual measured current. It is mainly caused by drift phenomena or residual current of current sensors or offset of operational amplifiers (op-amps) and A/D converters in the measuring circuits. The scaling error means nonideal scaling gain for phase current, which usually results from the unequal gains of the two current measurement channels, including current sensors, op-amps, and inaccuracy of passive elements in the measuring circuits. Considering both measurement errors, measured phase currents can be represented as follows:

$$i_{xs\_\mathrm{mea}} = K_x i_{xs} + I_{xs\_\mathrm{off}}. \tag{1}$$

In (1), nonunity K_x or nonzero I_{xs_off} implies the phase current measurement error, and the phase current measurement error can be defined as follows:

$$\Delta i_{xs} \equiv i_{xs\_\mathrm{mea}} - i_{xs}. \tag{2}$$

Considering a three-phase PMSM drive system with two phase current sensors, the measured currents can be presented, under that assumption of the measurement of a- and b-phase currents, as follows:

$$\begin{aligned} i_{as\_\mathrm{mea}} &= i_{as} + \Delta i_{as} \\ i_{bs\_\mathrm{mea}} &= i_{bs} + \Delta i_{bs} \\ i_{cs\_\mathrm{mea}} &= -\left(i_{as\_\mathrm{mea}} + i_{bs\_\mathrm{mea}}\right) \\ &= i_{cs} - (\Delta i_{as} + \Delta i_{bs}). \end{aligned} \tag{3}$$

Then, the previous phase currents can be denoted in the synchronous reference frame as (4a) and (4b), shown on the bottom of the page. The voltage model equations of a PMSM in the synchronous reference frame can be derived as follows:

$$\begin{aligned} v_{ds}^e &= R_s i_{ds}^e + L_d \frac{d}{dt} i_{ds}^e - \omega_r L_q i_{qs}^e \\ v_{qs}^e &= R_s i_{qs}^e + L_q \frac{d}{dt} i_{qs}^e + \omega_r \left(\lambda_f + L_d i_{ds}^e\right) \end{aligned} \tag{5}$$

where v_{ds}^e, v_{qs}^e, i_{ds}^e, i_{qs}^e, L_d, L_q, R_s, λ_f, and ω_r are the synchronous reference frame's d- and q-axis voltage, current, inductance, stator resistance, flux linkage generated by the permanent magnet of the rotor, and the rotational speed in electrical angle, respectively. Substituting (4a) into (5), the voltage model considering the current measurement error can be derived as follows:

$$\begin{aligned} v_{ds}^e &= R_s i_{ds\_\mathrm{mea}}^e + L_d \frac{d}{dt} i_{ds\_\mathrm{mea}}^e - \omega_r L_q i_{qs\_\mathrm{mea}}^e - \Delta v_{ds}^e \\ v_{qs}^e &= R_s i_{qs\_\mathrm{mea}}^e + L_q \frac{d}{dt} i_{qs\_\mathrm{mea}}^e \\ &\quad + \omega_r \left(\lambda_f + L_d i_{ds\_\mathrm{mea}}^e\right) - \Delta v_{qs}^e \end{aligned} \tag{6a}$$

$$\begin{aligned} \Delta v_{ds}^e &\equiv R_s \Delta i_{ds}^e + L_d \frac{d}{dt} \Delta i_{ds}^e - \omega_r L_q \Delta i_{qs}^e \\ \Delta v_{qs}^e &\equiv R_s \Delta i_{qs}^e + L_q \frac{d}{dt} \Delta i_{qs}^e + \omega_r L_d \Delta i_{ds}^e. \end{aligned} \tag{6b}$$

The last terms in the d- and q-axes in (6a) are originated from the current measurement error. These terms are defined as "voltage error" in this paper. The relationship between the voltage error and the current measurement error is shown in (6b). The voltage error is used to compensate the current measurement error, and it can be estimated with the commanded voltage reference of the current controller. When the conventional synchronous frame proportional-plus-integral (PI) current controller [9] is used as the current regulator, the cross-coupling and back-electromotive-force terms [the third terms in (6a)] are compensated with the feedforwarding terms, and the remainder of the equation is covered by the PI controller. Assuming that the time derivative of d- and q-axis currents is small enough to neglect, the voltage error can be estimated by subtracting the voltage drop of the resistance from the output of the PI controller, as follows:

$$\begin{aligned} \Delta v_{ds}^e &\approx -\left(v_{ds\_\mathrm{PI}}^e - \hat{R}_s i_{ds\_\mathrm{mea}}^e\right) \\ \Delta v_{qs}^e &\approx -\left(v_{qs\_\mathrm{PI}}^e - \hat{R}_s i_{qs\_\mathrm{mea}}^e\right) \end{aligned} \tag{7}$$

$$\begin{bmatrix} i_{ds\_\mathrm{mea}}^e \\ i_{qs\_\mathrm{mea}}^e \end{bmatrix} = \begin{bmatrix} \cos\theta_e & \cos\left(\theta_e - \frac{2}{3}\pi\right) & \cos\left(\theta_e + \frac{2}{3}\pi\right) \\ -\sin\theta_e & -\sin\left(\theta_e - \frac{2}{3}\pi\right) & -\sin\left(\theta_e + \frac{2}{3}\pi\right) \end{bmatrix} \begin{bmatrix} i_{as\_\mathrm{mea}} \\ i_{bs\_\mathrm{mea}} \\ i_{cs\_\mathrm{mea}} \end{bmatrix} = \begin{bmatrix} i_{ds}^e + \Delta i_{ds}^e \\ i_{qs}^e + \Delta i_{qs}^e \end{bmatrix} \tag{4a}$$

$$\begin{aligned} \Delta i_{ds}^e &= \Delta i_{as} \cos\theta_e + \frac{1}{\sqrt{3}} (\Delta i_{as} + 2\Delta i_{bs}) \sin\theta_e \\ \Delta i_{qs}^e &= -\Delta i_{as} \sin\theta_e + \frac{1}{\sqrt{3}} (\Delta i_{as} + 2\Delta i_{bs}) \cos\theta_e \end{aligned} \tag{4b}$$

where $v^e_{ds\_\mathrm{PI}}$ and $v^e_{qs\_\mathrm{PI}}$ stand for the output voltage reference of the d- and q-axis PI controller. $\hat{R}_s$ indicates the estimated stator resistance used in the current controller.

III. Compensation Strategy

This paper detects and compensates the current measurement error by manipulating the voltage error. The offset and the scaling error affect the voltage error independently, so that the two errors can be handled separately.

A. Offset Error

The offset error can be modeled as a constant phase current measurement error, as follows:

$$\begin{aligned}\Delta i_{as} &= I_{as\_\mathrm{off}} \\ \Delta i_{bs} &= I_{bs\_\mathrm{off}}.\end{aligned} \tag{8}$$

The previous error can be presented in the synchronous frame, by substituting (8) into (4b), and then, the voltage error caused by this current measurement error can be deduced by substituting (9) into (6b), as follows:

$$\begin{aligned}\Delta i^e_{ds} &= I_{\mathrm{off}} \sin(\theta_e - \varphi_{\mathrm{off}}) \\ \Delta i^e_{qs} &= I_{\mathrm{off}} \cos(\theta_e - \varphi_{\mathrm{off}})\end{aligned} \tag{9}$$

$$\begin{aligned}\Delta v^e_{ds} &= I_{\mathrm{off}} R_s \sin(\theta_e - \varphi_{\mathrm{off}}) \\ &\quad + I_{\mathrm{off}} \omega_r (L_d - L_q) \cos(\theta_e - \varphi_{\mathrm{off}}) \\ \Delta v^e_{qs} &= I_{\mathrm{off}} R_s \cos(\theta_e - \varphi_{\mathrm{off}}) \\ &\quad + I_{\mathrm{off}} \omega_r (L_d - L_q) \sin(\theta_e - \varphi_{\mathrm{off}})\end{aligned} \tag{10}$$

where

$$\begin{aligned}I_{\mathrm{off}} &= \sqrt{\Delta i^2_{as} + (\Delta i_{as} + 2\Delta i_{bs})^2} \\ \varphi_{\mathrm{off}} &= \tan^{-1}\left(\frac{-\Delta i_{as}}{\Delta i_{as} + 2\Delta i_{bs}}\right).\end{aligned}$$

As shown in (10), the voltage error terms are ac signals in the synchronous reference frame, which are associated with the magnitude and the phase information of the current measurement error. The voltage error has positive and negative sequence components with the synchronous frequency in the synchronous reference frame, and the current measurement error can be estimated from either the negative or positive sequence component of the voltage error by separating each sequence component, as follows:

$$\begin{bmatrix}\Delta i^e_{ds} \\ \Delta i^e_{qs}\end{bmatrix} \approx \begin{bmatrix}\cos\theta_e & \sin\theta_e \\ -\sin\theta_e & \cos\theta_e\end{bmatrix} \times \frac{1}{R_s}\mathrm{LPF}\left\{\begin{bmatrix}\cos\theta_e & -\sin\theta_e \\ \sin\theta_e & \cos\theta_e\end{bmatrix}\begin{bmatrix}\Delta v^e_{ds} \\ \Delta v^e_{qs}\end{bmatrix}\right\} \tag{11a}$$

$$\begin{bmatrix}\Delta i^e_{ds} \\ \Delta i^e_{qs}\end{bmatrix} \approx \begin{bmatrix}\cos\theta_e & \sin\theta_e \\ -\sin\theta_e & \cos\theta_e\end{bmatrix} \frac{1}{\omega_r(L_d - L_q)}\mathrm{LPF} \times \left\{\begin{bmatrix}0 & 1 \\ 1 & 0\end{bmatrix}\begin{bmatrix}\cos\theta_e & \sin\theta_e \\ -\sin\theta_e & \cos\theta_e\end{bmatrix}\begin{bmatrix}\Delta v^e_{ds} \\ \Delta v^e_{qs}\end{bmatrix}\right\} \tag{11b}$$

where $\mathrm{LPF}\{\cdot\}$ means that the value inside the curly brackets is processed through a low-pass filter (LPF). Equation (11a) explains how to obtain the current measurement error from the negative sequence component of the voltage error. In order to isolate the negative sequence component, the voltage error is rotated to the negative sequence reference frame. Then, the rotated signal is processed by an LPF after being divided by the stator resistance. Then, only the negative sequence component would remain. Finally, the current measurement error in the rotor reference frame can be obtained by rotating the processed signal to the synchronous reference frame, again. The current measurement error can be also estimated from the positive sequence component in a similar way, as shown in (11b). The voltage error is rotated to the positive sequence reference frame and input to the LPF after being divided by the product of rotational speed and the d- and q-axis inductance difference to extract only the positive sequence component. Rotating the processed signal to the synchronous reference frame again results in the current measurement error.

Fig. 1 shows the block diagram of the proposed offset error compensator in vector form. The anti-diagonal matrix in (11b) is presented by the composition of a complex conjugation and unit imaginary number. It estimates the current measurement error with the voltage error and compensates it to the measured current. Theoretically, the current measurement error can be obtained with either the positive or negative sequence component of the voltage error. However, magnitudes of the negative and positive sequence components of the voltage error are dependent on the machine parameters and operating conditions. The magnitude of the negative sequence component is larger than that of the positive sequence component in low-speed range, and vice versa in high-speed range. In order to exploit relatively high-level signal and enhance the signal-to-noise ratio, a linear combination method is employed. After negative and positive sequence components of the voltage error are extracted, weighting factors are applied to them. The weighting factors are set to reflect the negative sequence component most in low-speed region and the positive sequence component most in high-speed region. The weighting factors are formulated as follows:

$$W_H = \begin{cases} 0, & |\omega_r| \le \omega_{\mathrm{low}} \\ \frac{|\omega_r| - \omega_{\mathrm{low}}}{\omega_{\mathrm{high}} - \omega_{\mathrm{low}}}, & \omega_{\mathrm{low}} < |\omega_r| \le \omega_{\mathrm{high}} \\ 1, & \omega_{\mathrm{high}} < |\omega_r| \end{cases}$$

$$W_L = \begin{cases} 1, & |\omega_r| \le \omega_{\mathrm{low}} \\ \frac{\omega_{\mathrm{high}} - |\omega_r|}{\omega_{\mathrm{high}} - \omega_{\mathrm{low}}}, & \omega_{\mathrm{low}} < |\omega_r| \le \omega_{\mathrm{high}} \\ 0, & \omega_{\mathrm{high}} < |\omega_r|. \end{cases} \tag{12}$$

When the rotational speed is lower than ω_{low}, only the negative sequence component is used, whereas only the positive sequence component is used when the rotational speed is higher than ω_{high}. A division by zero at standstill can be prevented by this scheme also.

In addition, an integrator is used to avoid the steady-state error before the rotating transformation to the synchronous reference frame. The estimated current measurement error is

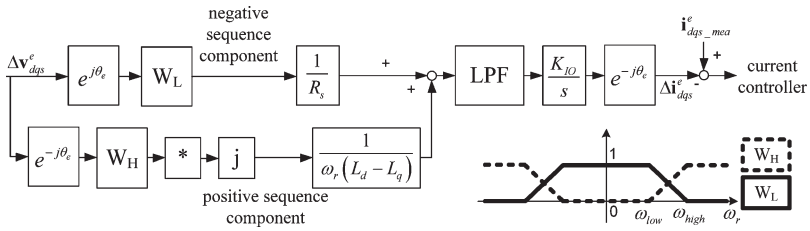

Fig. 1. Block diagram of the offset error compensator.

subtracted from the measured current, and the compensated current is used as the input to the current controller.

B. Scaling Error

Scaling error occurs when at least one of the scaling gains is not accurate. However, even if the scaling error exists, the measured phase currents could be kept as almost sinusoidal since the current controller would regulate them, as follows:

$$\begin{aligned} i_{as\_\mathrm{mea}} &= K_a i_{as} = I\cos(\theta_e+\phi) \\ i_{bs\_\mathrm{mea}} &= K_b i_{bs} = I\cos\left(\theta_e-\frac{2}{3}\pi+\phi\right) \end{aligned} \tag{13}$$

where $\phi=\tan^{-1}(i^e_{qs\_\mathrm{mea}}/i^e_{ds\_\mathrm{mea}})$, and I is the magnitude of the measured current. Considering the nonunity scaling gains and using the definition in (2), the current measurement error in the abc frame and in the synchronous reference frame can be derived as follows:

$$\begin{aligned} \Delta i_{as} &= I\left(1-\frac{1}{K_a}\right)\cos(\theta_e+\phi) \\ \Delta i_{bs} &= I\left(1-\frac{1}{K_b}\right)\cos\left(\theta_e-\frac{2}{3}\pi+\phi\right) \end{aligned} \tag{14a}$$

$$\begin{aligned} \Delta i^e_{ds} = \frac{I}{\sqrt{3}}\Bigg\{ &\left(\frac{1}{K_b}-\frac{1}{K_a}\right)\sin\left(2\theta_e+\frac{\pi}{3}+\phi\right) \\ &+\left(1-\frac{1}{K_a}\right)\sin\left(\frac{\pi}{3}-\phi\right) \\ &+\left(1-\frac{1}{K_b}\right)\sin\left(\frac{2\pi}{3}-\phi\right)\Bigg\} \\ \Delta i^e_{qs} = \frac{I}{\sqrt{3}}\Bigg\{ &\left(\frac{1}{K_b}-\frac{1}{K_a}\right)\cos\left(2\theta_e+\frac{\pi}{3}+\phi\right) \\ &+\left(1-\frac{1}{K_a}\right)\cos\left(\frac{\pi}{3}-\phi\right) \\ &+\left(1-\frac{1}{K_b}\right)\cos\left(\frac{2\pi}{3}-\phi\right)\Bigg\}. \end{aligned} \tag{14b}$$

Equation (14b) shows that the current measurement error caused by the scaling error contains negative sequence component at two times of the synchronous frequency and dc component. Since the voltage error and the current measurement have linear relationship, as shown in (6b), the voltage error also consists of the ac component with two times of the synchronous frequency and dc component. Among them, the ac component of the voltage error can be derived as follows:

$$\begin{aligned} \Delta v^e_{ds} &= \Delta v^e_{ds\_\mathrm{neg}} + \Delta v^e_{ds\_\mathrm{pos}} \\ \Delta v^e_{qs} &= \Delta v^e_{qs\_\mathrm{neg}} + \Delta v^e_{qs\_\mathrm{pos}} \end{aligned} \tag{15a}$$

$$\begin{aligned} \Delta v^e_{ds\_\mathrm{neg}} &= \frac{I}{\sqrt{3}}\left(\frac{1}{K_b}-\frac{1}{K_a}\right)\sqrt{R_s^2+\{0.5\omega_r(L_d+L_q)\}^2} \\ &\quad\times\sin(2\theta_e+\theta_{\mathrm{neg}}) \\ \Delta v^e_{qs\_\mathrm{neg}} &= \frac{I}{\sqrt{3}}\left(\frac{1}{K_b}-\frac{1}{K_a}\right)\sqrt{R_s^2+\{0.5\omega_r(L_d+L_q)\}^2} \\ &\quad\times\cos(2\theta_e+\theta_{\mathrm{neg}}) \end{aligned} \tag{15b}$$

$$\begin{aligned} \Delta v^e_{ds\_\mathrm{pos}} &= \frac{I\sqrt{3}}{2}\left(\frac{1}{K_b}-\frac{1}{K_a}\right)\omega_r(L_d-L_q) \\ &\quad\times\cos\left(2\theta_e+\frac{\pi}{3}+\phi\right) \\ \Delta v^e_{qs\_\mathrm{pos}} &= \frac{I\sqrt{3}}{2}\left(\frac{1}{K_b}-\frac{1}{K_a}\right)\omega_r(L_d-L_q) \\ &\quad\times\sin\left(2\theta_e+\frac{\pi}{3}+\phi\right) \end{aligned} \tag{15c}$$

where $\theta_{\mathrm{neg}}=(\pi/3)+\phi+\tan^{-1}\{0.5\omega_r(L_d+L_q)/R_s\}$. The ac component of the voltage error has the positive and negative sequence components of twice the synchronous frequency in the synchronous reference frame. Although both the positive and negative sequence components of the voltage error include the information of the current measurement error, this paper exploits only the negative sequence component, i.e., (15b), since it persists regardless of operating speed, whereas the positive sequence component, i.e., (15c), converges into zero as the rotational speed decreases. In particular, in the case of surface-mount permanent-magnet synchronous motor, the coefficient of the positive sequence component is null at any speed because of equal inductance values in the d- and q-axes.

In the previous section, the proposed offset error compensator estimates the current measurement error and compensates it directly. However, the scaling error compensation is achieved in a different way. Using the negative sequence component of the voltage error, the scaling gain difference $((1/K_b)-(1/K_a))$ is estimated, and the estimated value modifies each phase's scaling gain to make the scaling gain difference zero.

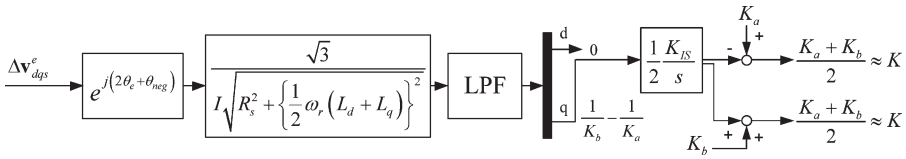

Fig. 2. Block diagram of the scaling error compensator.

Being analogous to the estimation process in (11a), the scaling gain difference can be estimated using

$$\begin{aligned}&\begin{bmatrix}0\\ \left(\frac{1}{K_b}-\frac{1}{K_a}\right)\end{bmatrix}\\ &\quad\approx \mathrm{LPF}\Bigg\{\frac{\sqrt{3}}{I\sqrt{R_s^2+\{0.5\omega_r(L_d+L_q)\}^2}}\\ &\qquad\times\begin{bmatrix}\cos(2\theta_e+\theta_{\mathrm{neg}}) & -\sin(2\theta_e+\theta_{\mathrm{neg}})\\ \sin(2\theta_e+\theta_{\mathrm{neg}}) & \cos(2\theta_e+\theta_{\mathrm{neg}})\end{bmatrix}\\ &\qquad\times\begin{bmatrix}\Delta v^e_{ds}\\ \Delta v^e_{qs}\end{bmatrix}\Bigg\}.\end{aligned}\tag{16}$$

Fig. 2 presents the block diagram of the proposed scaling error compensator. The reference frame rotation, gain multiplication, and filtering process are applied to the voltage error, successively. Then, the scaling gain difference can be acquired in the q-axis of the resultant signal, and an integrator is employed for this signal in order to suppress the steady-state error. Afterward, the acquired scaling gain error is applied to the phase scaling gains K_a and K_b for gain compensation. With an assumption that K_a and K_b are nearly one, the scaling gains are compensated as follows:

$$\begin{aligned}K_a-\frac{1}{2}\left(\frac{1}{K_b}-\frac{1}{K_a}\right)&=K_a-\frac{1}{2}\frac{K_a-K_b}{K_aK_b}\\ &\approx K_a-\frac{1}{2}(K_a-K_b)=\frac{1}{2}(K_a+K_b)\\ K_b+\frac{1}{2}\left(\frac{1}{K_b}-\frac{1}{K_a}\right)&=K_b+\frac{1}{2}\frac{K_a-K_b}{K_aK_b}\\ &\approx K_b+\frac{1}{2}(K_a-K_b)\\ &=\frac{1}{2}(K_a+K_b).\end{aligned}\tag{17}$$

Assuming that the scaling error compensator estimates and compensates the scaling gain error well, two scaling gains become identical eventually, i.e., $K_a=K_b$. Then, the ac component of current measurement error in the rotor reference frame would vanish. However, there still might be the dc component error.

C. Limitation on Scaling Error Compensation

The scaling error compensator shown in Fig. 2 only compensates the scaling gain difference. Therefore, the compensated scaling gain may not be unity $((K_a+K_b/2)\neq 1)$, and the voltage error would have the dc component, which can be derived as follows:

$$\begin{aligned}\Delta v^e_{ds}&=\left(1-\frac{1}{K}\right)I\sqrt{R_s^2+(\omega_rL_q)^2}\\ &\quad\times\sin\left(-\phi+\tan^{-1}\left(\frac{R_s}{\omega_rL_q}\right)\right)\\ \Delta v^e_{qs}&=\left(1-\frac{1}{K}\right)I\sqrt{R_s^2+(\omega_rL_d)^2}\\ &\quad\times\sin\left(\phi+\tan^{-1}\left(\frac{\omega_rL_q}{-R_s}\right)\right)\end{aligned}\tag{18}$$

where the average scaling gain $K=(K_a+K_b/2)$. Theoretically, the average scaling gain K can be calculated from (18). The calculation of K might be a similar process to that used for the estimation of the scaling gain difference. However, it is difficult to compensate to the average scaling gain because the output voltage of the PI controller may also contain dc component originated from other sources, e.g., inaccurate or varying machine parameters. In addition, the effect of the average scaling error on the voltage error is usually smaller than that of the parameter error. Therefore, the average scaling error terms cannot be isolated from the whole dc component of the voltage error.

The average scaling error causes the dc component of the current measurement error in the synchronous reference frame, which results in the torque offset. That means the effect of the average scaling error is similar to that of the parameter error. The variation of the inductance or the flux linkage also causes the torque offset from the designed value. Therefore, sometimes, the average scaling error does not need to be distinguished from the parameter error. Instead, it may be compensated by torque reference modification in the outer control loop, such as a speed control loop. Otherwise, the average scaling error is only monitored. It can be regarded as a fault if the average scaling error exceeded a certain critical level.

On the other hand, the offset error and the scaling gain difference cause the independent voltage error signals with their own characteristic frequencies in the synchronous reference frame, which induce the torque fluctuation. These two kinds of measurement errors are compensated by the proposed compensator. Fig. 3 shows the block diagram of an entire drive system with the proposed current measurement error compensator. The offset error is directly compensated, and the scaling gain difference is compensated by adjusting the phase scaling gains.

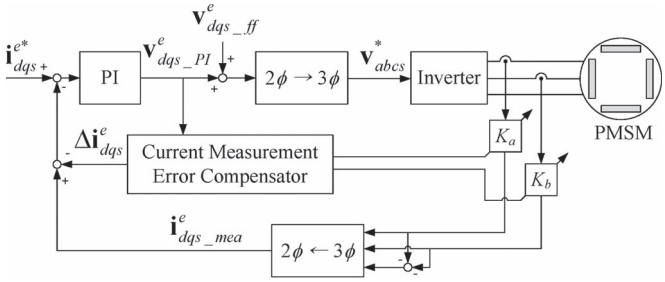

Fig. 3. Block diagram of the current-controlled drive system integrated with the measurement error compensator.

TABLE I
PARAMETERS OF THE TEST MOTOR

Quantity	Value [Unit]
Number of pole	4
Phase resistance	R_s; 0.265 [Ω]
Inductance	L_d; 3.66 [mH] L_q; 7.22 [mH]
Rotor flux linkage	λ_f; 0.18 [Vs]
Rated current	23.8 [A_{peak}]
Rated torque	12.7 [Nm]
Rated speed	5000 [r/min]

D. Practical Issues

The proposed method is based on the specific patterns on the voltage error caused by the current measurement error. Since the actual terminal motor voltage is usually not able to measure, the voltage error is estimated with the commanded voltage of the current controller, as shown in (7). However, the estimated voltage error can be inaccurate due to some factors.

First, the motor parameters vary according to the operating conditions. The stator resistance varies in accordance with the stator winding temperature, and the inductance also varies by the magnetic saturation of motor core. Since the proposed method utilizes the motor model to estimate the voltage error, it is affected by the motor parameter error or parameter variation. The resistance is used in (7) to estimate the voltage error. The inductance is used to make the feedforwarding terms in (6a). If there were difference between actual and estimated inductance values, it would affect the commanded voltage of the current controller and, thus, the estimated voltage error in (7).

However, variation of the parameter occurs independently of the synchronous frequency. The winding temperature varies slowly compared to the synchronous frequency, and the effect of this on the voltage error is not related to the synchronous frequency. The extent of the inductance saturation depends on the amount of current flowing on the motor winding. Since the inductance value is used to calculate the feedforwarding terms, the effect on voltage error by the inductance variation is related to the load and the speed pattern, not the synchronous frequency. Since the proposed method extracts and employs only specific synchronous-frequency-related components, the effect of the parameter variation on the voltage error can be filtered out. Simple parameter error would also be filtered out in the same manner and only affect the convergence dynamics since the parameters are used as gains in the proposed method, as shown in Figs. 1 and 2.

Second, the effective voltage applied to the motor terminals might be different from the commanded voltage of the current controller, due to the voltage distortion of the inverterlike nonlinear voltage drop of the semiconductor, dead time, etc. [14], [15]. However, the voltage distortion by the inverter is mainly composed of sixth harmonics in the synchronous reference frame, which is not used in the proposed method. Therefore, the effect of the voltage distortion on the voltage error can be filtered out also.

Some kinds of motor faults (bearing faults, eccentricity-related faults, interturn short of stator windings, and so on) cause harmonics with multiples of the synchronous frequency [16]. Some researches have been presented to detect the motor faults [17], [18]. They usually monitor certain harmonic signals as fault indicators. Since the proposed method also uses these harmonic components to compensate the current measurement error, it is required to distinguish the motor faults from the current measurement error.

If motor faults occurred, harmonics components would be caused on the commanded voltage of the current controller, and both the motor fault detection algorithm and the proposed compensation method would react to them. However, dynamics of the motor fault detection should be much faster than that of the proposed compensation method because the motor faults are the more urgent problem than the current measurement error. For example, once the interturn fault occurs, the excessive fault current begins flowing through the faulty windings, and the fault develops into a serious failure of the motor. In addition, these kinds of faults occur in a sudden manner, so that the detection should be done as soon as the faults occur and a proper action should be performed immediately to protect the motor. On the other hand, the current measurement error tends to progress more gradually; hence, it does not need to be compensated so immediately. Rather, it had better set the dynamics of the current measurement error compensator slow to make it not too sensitive to noise. Eventually, the motor faults can be separated from the current measurement error by adjusting the dynamics of the motor fault detection method fast enough.

IV. EXPERIMENTAL RESULTS

Experiments were performed to verify the effectiveness of the operation of the proposed compensator. An interior PMSM coupled with a load machine was used for the test. The motor under test governed the load torque, and the rotating speed was controlled by the load machine. Both the test motor and the load machine are operated by three-phase inverters using insulated-gate bipolar transistors. All the motor control and the compensation of the current measurement errors were achieved with a commercial digital signal processor controller (TMS320F28335, Texas Instruments Incorporated). Parameters for the test motor are shown in Table I.

Fig. 4 shows the current control performance. Since the proposed method depends on the commanded voltage reference of the current controller, the performance of the current controller

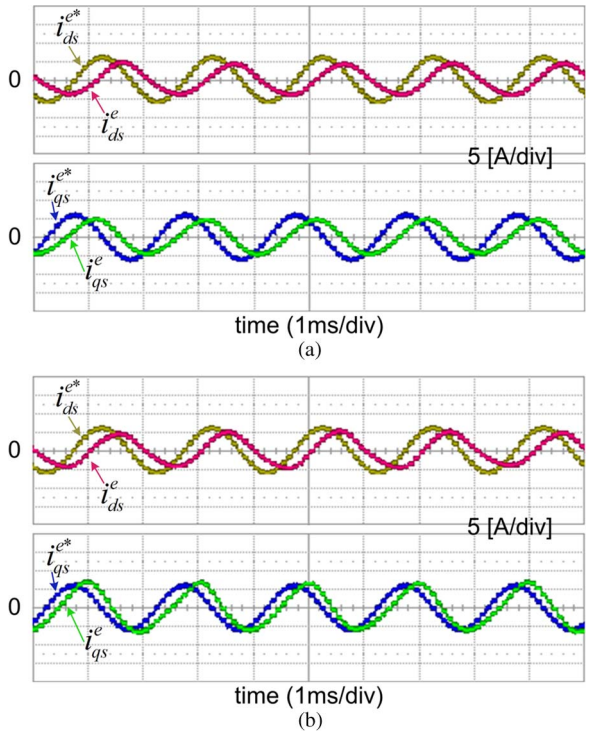

Fig. 4. Current control performance. (a) Without parameter errors. (b) With parameter errors.

TABLE II
PARAMETERS OF THE CURRENT CONTROLLER

Quantity	Value [Unit]
Bandwidth	500 [Hz]
Switching frequency	10 [kHz]
Estimated phase resistance	$\hat{R}_s$; 0.186 [Ω] $(0.7R_s)$
Estimated inductance	$\hat{L}_d$; 4.03 [mH] $(1.1L_d)$
	$\hat{L}_q$; 14.44 [mH] $(2L_q)$

is important. That is, the bandwidth of the current controller should be wide enough compared to the synchronous frequency.

The synchronous reference frame PI controller was used for the current control. In order to investigate the effect of the parameter error, current control results with correct and incorrect motor parameters are compared. The bandwidth and the incorrect motor parameters used for the current controller are shown in Table II. The current references were set as follows:

$$i_{ds}^{e*} = 6\sin(2\pi 500t)$$
$$i_{qs}^{e*} = 6\cos(2\pi 500t). \tag{19}$$

In Fig. 4(a), it is shown that the actual d- and q-axis currents follow their reference well according to the set bandwidth. The performance of the current controller got worse a bit with the parameter errors, as shown in Fig. 4(b). Some high-frequency components are shown on the actual d- and q-axis currents, but still the fundamental frequency component (500 Hz) seems to be regulated to some degree. Since the frequency of the signal handled by the proposed current error compensation method is lower than this frequency, the performance of the current controller can be regarded enough to be used.

TABLE III
OPERATING CONDITION AND INTENTIONALLY INSERTED MEASUREMENT ERROR

Quantity	Value [Unit]
Rotational speed	1500 [r/min]
Load torque	9.3 [Nm]
I_{as_off}	0.3 [A]
I_{bs_off}	-0.2 [A]
K_a	1.01
K_b	0.98
K_{IS}	0.1
K_{IO}	0.4

In order to verify the relationship between the voltage error and the current measurement error, the voltage error was observed while the measurement error was inserted intentionally. Operating conditions and the inserted measurement error are shown in Table III. The whole current measuring range of the system is 50 A. Under the consideration of the measurement range, it can be said that the current measurement error condition used in the experiment is quite small enough to check the sensitivity of the proposed compensation method.

Fig. 5 shows the voltage error spectrum with and without the parameter errors and the current measurement errors. It is clearly shown that the synchronous frequency (50 Hz) and twice of the synchronous frequency (100 Hz) component were found much more when the measurement errors were inserted than when the measurement errors were not inserted. These results coincide with the derived voltage error caused by the measurement errors shown in (10) and (15). In addition, the parameter error does not affect the voltage error much.

Fig. 6 shows operation of the proposed compensator under the current measurement errors in a steady state, with and without the parameter errors. The extent of parameter errors was set, as shown in Table II. The current measurement error in the synchronous reference frame and the scaling gains are represented. The operating condition and the inserted measurement error are shown in Table III. While the rotor was rotating at steady state with the load torque, the measurement error was inserted in a step manner. After the measurement errors were inserted, the ac component of the current measurement error gradually converged to an acceptable level. Both scaling gains converged to 0.995, which makes the scaling gain difference zero. Since the average scaling gain is not compensated, there existed small dc error in the current measurement error. The parameter error barely affected the operation of the proposed compensator. As explained in Section III, its effect on the voltage error was filtered out, unless the parameter varies with the synchronous frequency. Only dynamic response was a bit different since the proposed compensation method uses the motor parameters as gains, as shown in Figs. 1 and 2

Fig. 7 shows operation of the proposed compensator under the current measurement error in a dynamic state. The rotating speed and load torque patterns are the scaled-down version of an operation profile of an electric vehicle traction system.

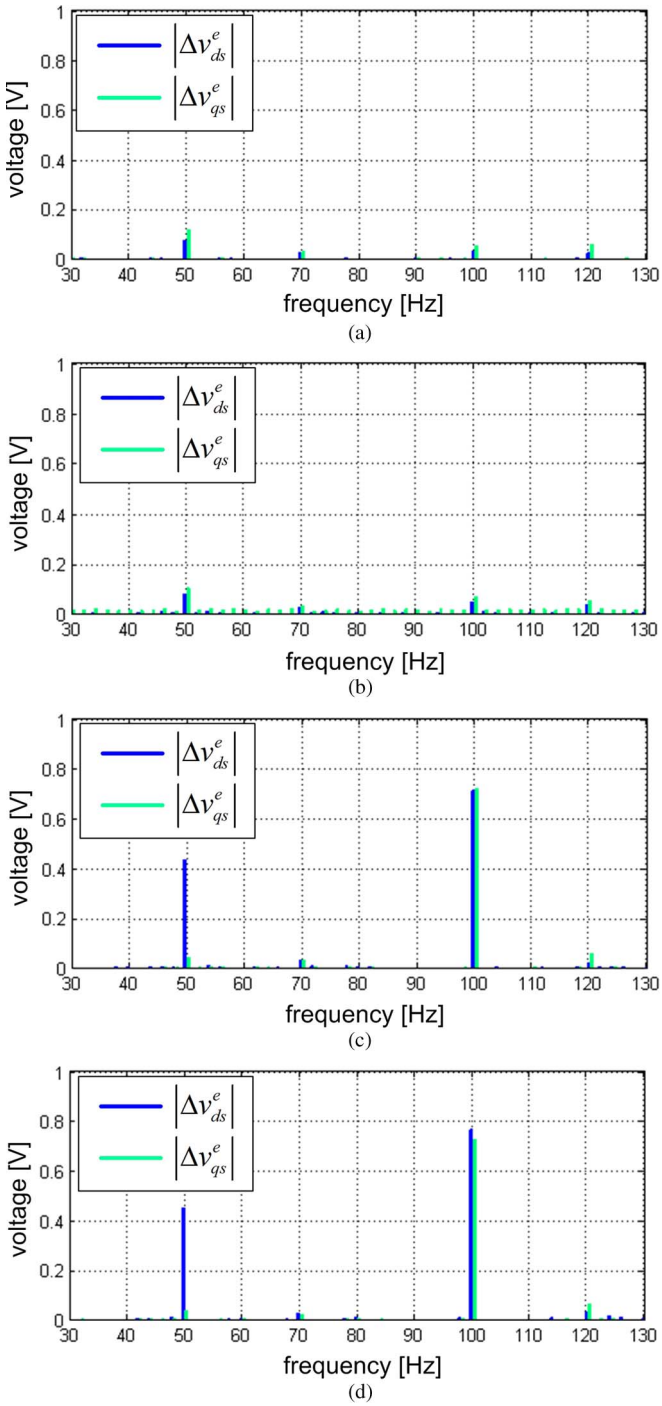

Fig. 5. Voltage error according to the parameter errors and the current measurement errors in the frequency domain. (a) Without parameter and measurement errors. (b) With parameter errors and without measurement errors. (c) Without parameter errors and with measurement errors. (d) With parameter and measurement errors.

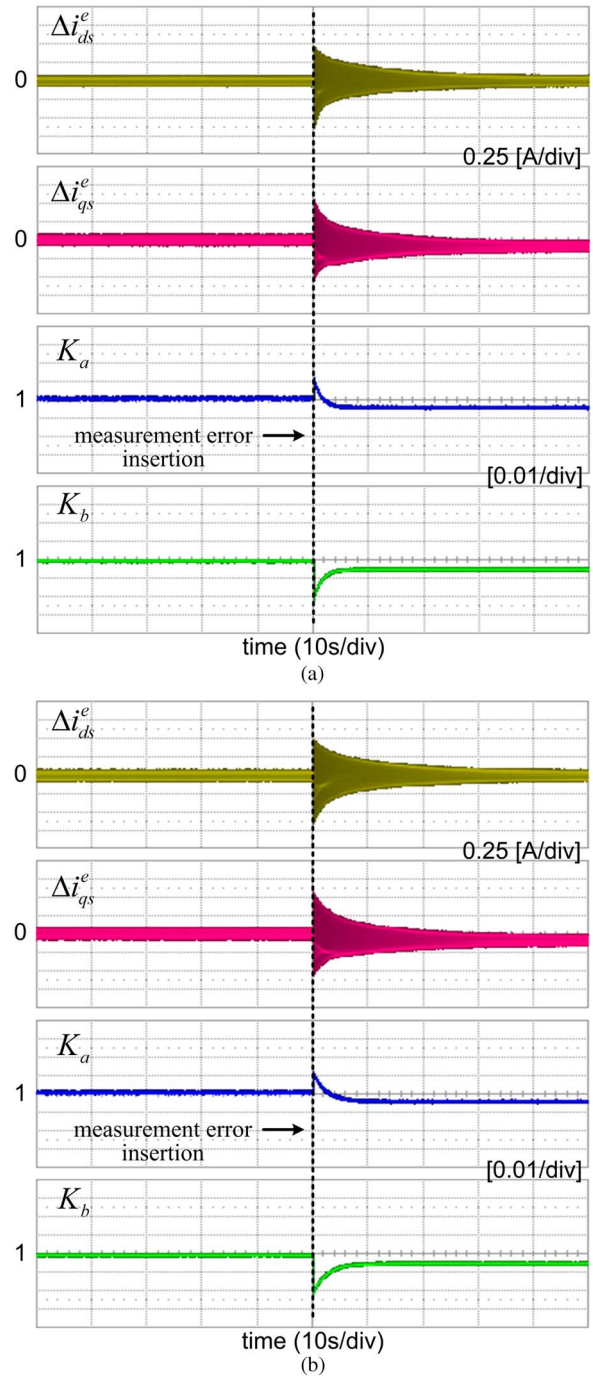

Fig. 6. Measurement error compensation response in steady state. (a) Without parameter errors. (b) With parameter errors.

The current measurement error in the synchronous reference frame and the rotational speed and load torque are plotted. During the operation, the measurement error with the condition in Table III was inserted. After the measurement error was inserted, the ac component of the current measurement error decreased gradually and was maintained in a reasonable range. When the load torque changed rapidly, the current measurement error increased transiently, since the time derivative term of the current is not considered in calculation of the voltage error. However, the LPF and the integrator of the proposed compensator filtered the transient miscalculation of the voltage error, satisfactorily.

V. Conclusion

A current measurement error compensation method has been presented in this paper. The proposed method is used for the current-controlled three-phase PMSM drive system with two phase current sensors. The current measurement error caused by the offset and the scaling error affects the commanded

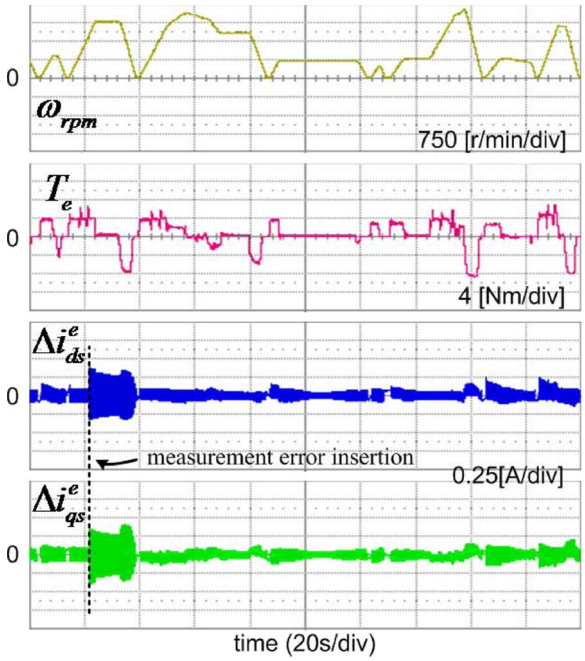

Fig. 7. Measurement error compensation response in dynamic state.

voltage reference of the PI current controller, which is defined as the voltage error. The proposed compensator exploits the voltage error to compensate the measurement error. Since the voltage errors caused by the offset error and the scaling gain difference have independent frequency characteristics, compensation of each component can be achieved separately. However, the voltage error caused by average scaling error is difficult to be isolated from the parameter error. The proposed compensation method has been confirmed with the experimental results. It is verified that the current measurement error causes the voltage error and the measurement errors have been well compensated and converged into the allowable range by the proposed compensator under steady-state and dynamic-state operation.

REFERENCES

[1] S.-H. Song, J.-W. Choi, and S.-K. Sul, "Digitally controlled AC drives," *IEEE Ind. Appl. Mag.*, vol. 6, pp. 51–62, 2000.
[2] G. Buja and R. Menis, "Steady-state performance degradation of a DTC IM drive under parameter and transduction errors," *IEEE Trans. Ind. Electron.*, vol. 55, no. 4, pp. 1749–1760, Apr. 2008.
[3] S. Suzuki and M. Yoshida, "Elevator control apparatus with compensation for current sensor offset voltage," U.S. Patent 5407027, 1995.
[4] Y. Okita, "Electric power conversion device," U.S. Patent 6 154 379, Nov. 28, 2000.
[5] D.-W. Chung and S.-K. Sul, "Analysis and compensation of current measurement error in vector-controlled AC motor drives," *IEEE Trans. Ind. Appl.*, vol. 34, no. 2, pp. 340–345, Mar./Apr. 1998.
[6] Q. Weizhe, S. K. Panda, and J.-X. Xu, "Torque ripple minimization in PM synchronous motors using iterative learning control," *IEEE Trans. Power Electron.*, vol. 19, no. 2, pp. 272–279, Mar. 2004.
[7] M. C. Harke, J. M. Guerrero, M. W. Degner, F. Briz, and R. D. Lorenz, "Current measurement gain tuning using high-frequency signal injection," *IEEE Trans. Ind. Appl.*, vol. 44, no. 5, pp. 1578–1586, Sep./Oct. 2008.
[8] M. C. Harke and R. D. Lorenz, "The spatial effect and compensation of current sensor gain deviation for three-phase three-wire systems," *IEEE Trans. Ind. Appl.*, vol. 44, no. 4, pp. 1181–1189, Jul./Aug. 2008.
[9] H.-S. Jung, S.-H. Hwang, J.-M. Kim, C.-U. Kim, and C. Choi, "Diminution of current-measurement error for vector-controlled AC motor drives," *IEEE Trans. Ind. Appl.*, vol. 42, no. 5, pp. 1249–1256, Sep./Oct. 2006.
[10] K. R. Cho and J. K. Seok, "Correction on current measurement errors for accurate flux estimation of ac drives at low stator frequency," *IEEE Trans. Ind. Appl.*, vol. 44, no. 2, pp. 594–603, Mar./Apr. 2008.
[11] K.-R. Cho and J.-K. Seok, "Pure-integration-based flux acquisition with drift and residual error compensation at a low stator frequency," *IEEE Trans. Ind. Appl.*, vol. 45, no. 4, pp. 1276–1285, Jul./Aug. 2009.
[12] Y.-S. Jeong, S.-K. Sul, S. E. Schulz, and N. R. Patel, "Fault detection and fault-tolerant control of interior permanent-magnet motor drive system for electric vehicle," *IEEE Trans. Ind. Appl.*, vol. 41, no. 1, pp. 46–51, Jan./Feb. 2005.
[13] T. R. Rowan and R. L. Kerkman, "A new synchronous current regulator and an analysis of current-regulated PWM inverters," *IEEE Trans. Ind. Appl.*, vol. IA-22, no. 4, pp. 678–690, Jul./Aug. 1986.
[14] J.-W. Choi and S.-K. Sul, "A new compensation strategy reducing voltage/current distortion in PWM VSI systems operating with low output voltages," *IEEE Trans. Ind. Appl.*, vol. 31, no. 5, pp. 1001–1008, Sep./Oct. 1995.
[15] H.-S. Kim, H.-T. Moon, and M.-J. Youn, "On-line dead-time compensation method using disturbance observer," *IEEE Trans. Power Electron.*, vol. 18, no. 6, pp. 1336–1345, Nov. 2003.
[16] S. Nandi, H. A. Toliyat, and L. Xiaodong, "Condition monitoring and fault diagnosis of electrical motors—A review," *IEEE Trans. Energy Convers.*, vol. 20, no. 4, pp. 719–729, Dec. 2005.
[17] B.-M. Ebrahimi and J. Faiz, "Feature extraction for short-circuit fault detection in permanent-magnet synchronous motors using stator-current monitoring," *IEEE Trans. Power Electron.*, vol. 25, no. 10, pp. 2673–2682, Oct. 2010.
[18] B. Akin, S. Choi, U. Orguner, and H. A. Toliyat, "A simple real-time fault signature monitoring tool for motor-drive-embedded fault diagnosis systems," *IEEE Trans. Ind. Electron.*, vol. 58, no. 5, pp. 1990–2001, May 2011.

Myoungho Kim (S'09–M'14) was born in Seoul, Korea, in 1984. He received the B.S. degree in electrical engineering from Hanyang University, Seoul, Korea, in 2006 and the M.S. and Ph.D. degrees in electrical engineering from Seoul National University, Seoul, Korea, in 2008 and 2013, respectively.

Since 2013, he has been a Manager with the Power and Control Division, Samsung Heavy Industries, Hwasung, Korea. His research interests include high-power motor drives and wind-power converters.

Seung-Ki Sul (S'78–M'80–SM'98–F'00) was born in Korea in 1958. He received the B.S., M.S., and Ph.D. degrees from Seoul National University, Seoul, Korea, in 1980, 1983, and 1986, respectively, all in electrical engineering.

From 1986 to 1988, he was an Associate Researcher with the Department of Electrical and Computer Engineering, University of Wisconsin–Madison, Madison, WI, USA. From 1988 to 1990, he was a Principal Research Engineer with Gold-Star Industrial Systems Company. Since 1991, he has been a Professor with the School of Electrical Engineering and Computer Science, Seoul National University, where he was the Vice Dean from 2005 to 2007 and the President of the Korea Electrical Engineering and Science Research Institute from 2008 to 2011. His current research interests are power-electronic control of electric machines, electric/hybrid vehicle drives, and power-converter circuits.

Junggi Lee (S'02–M'09) was born in Jeonju, Korea, in 1975. He received the B.S. degree in control and instrumentation engineering from Chonbuk National University, Jeonju, Korea, in 2002 and the M.S. and Ph.D. degrees in electrical engineering from Pohang University of Science and Technology (POSTECH), Pohang, Korea, in 2004 and 2009, respectively.

He is currently a Working Part Leader in the inverter area of the Power Electronics Team, LG Electronics, Incheon, Korea. His current research interests include design, analysis, and control of power electronic systems and traction motor drives for hybrid and electric vehicles.